

CHARACTERIZATION OF ACACIA MANGIUM WOOD BASED ACTIVATED CARBONS PREPARED IN THE PRESENCE OF BASIC ACTIVATING AGENTS

Mohammed Danish,^{a,*} Rokiah Hashim,^a M. N. Mohamad Ibrahim,^b Mohd Rafatullah,^a Tanweer Ahmad,^a and Othman Sulaiman^a

The aim of this study was to observe the effects of alkaline activating agents on the characteristics, composition, and surface morphology of the designed activated carbons. Activated carbons were prepared by pyrolysis of *Acacia mangium* wood in the presence of two basic activating agents (calcium oxide and potassium hydroxide). The extent of impregnation ratio of precursor to activating agents was fixed at 2:1(w/w). Prior to pyrolysis, 24 hours soaking was conducted at 348 K. Activation was carried out in a stainless steel capped graphite crucible at 773 K for 2 hours in the absence of purge gas. The burn-off percentage was found to be 70.27±0.93% for CaO activated carbon (COAC) and 73.30±0.20% for KOH activated carbon (PHAC). The activating agents had a strong influence on the surface functional groups as well as elemental composition of these activated carbons. Characterization of the activated carbon obtained was performed with field emission scanning electron microscopy (FESEM), energy dispersive X-ray spectroscopy (EDX), Fourier transform infrared spectroscopy (FTIR), thermogravimetric analysis (TGA), and nitrogen adsorption as Brunauer, Emmett and Teller (BET) and Dubinin-Radushkevich (DR) isotherms.

Keywords: Activated carbon; *Acacia mangium*; Pyrolysis; Chemical activation; Calcium oxide; Potassium hydroxide

Contact information: a: School of Industrial Technology, Universiti Sains Malaysia 11800 Penang, Malaysia; b: School of Chemical Science, Universiti Sains Malaysia 11800 Penang, Malaysia;
* Corresponding author: mdanishchem@gmail.com

INTRODUCTION

Activated carbon has received much attention in the recent past due to its versatile application in material science, fulfilling various criteria needed for new materials. Activated carbon is the final product of an activation process of carbonaceous materials from different sources and with a carbon content in the range 70 to 90%. An activated carbon includes a wide range of amorphous-based materials prepared to exhibit a high degree of porosity and an extended inter-particulate surface area. An activated carbon with excellent adsorbent characteristics can be useful for a wide variety of processes including filtration, purification, deodorization, decolouration, and separation (Bansal et al. 1988). The physical properties and the chemical composition of the precursor, as well as the methods and process conditions employed for activation determine the final pore size distribution and the adsorption properties of the activated carbon (Bota et al. 1997).

The processes used for activation are broadly divided into two categories, physical activation and chemical activation. In a physical activation process steam or carbon dioxide are used for mild oxidation of the carbonaceous matter. The process is usually carried out in two stages. The first stage is the carbonization, and this is followed by an activation stage. In a chemical activation process dehydrating agents are used, such as H_2SO_4 (Hameed et al. 2007), H_3PO_4 (Solum et al. 1995), KOH (Jagtøyen and Derbyshire 1998), ZnCl_2 (Moreno-Pirajan and Giraldo 2010), or CaO (Danish et al. 2010).

Activated carbon can be defined by its properties as well as by its source. It can be produced from almost any organic substance having a high carbon content. Many agricultural products and by-products have been used as a source for activated carbon. From plantation trees in particular not much work has been reported. Activation of white oak wood with orthophosphoric acid and its effect on the structure of developed activated carbon structure through ^{13}C -NMR & FTIR studies has been reported by Solum et al. (1995). Subsequent work with white oak has been extended to include yellow poplar wood (Jagtøyen and Derbyshire 1998). A possible mechanism to explain phosphoric acid activation, as well as the use of phosphorus compounds as fire retardants for wood and cellulose, has been reported by Jagtøyen and Derbyshire (1998). Lee and Reucroft (1999) reported the comparative study of oak tree (hardwood) and coal based KOH and H_3PO_4 activated carbons. Patnukao and Pavasant (2008) reported activation of *Eucalyptus camaldulensis dehn* bark with orthophosphoric acid. A mixture of wood has been activated with $\text{H}_3\text{PO}_4/[(\text{NH}_4)_2\text{HPO}_4]$ by Benadi et al. (2000). An attempt has been made to produce activated carbon from tamarind wood by Kumar et al. (2010) at a carbonization temperature of 500 °C for 60 minutes and activating agent to precursor ratio fixed at 100%. The author found that the produced activated carbon had a surface area (using the Brunauer, Emmett and Teller, BET method) of 1240 m^2/g and characterised surface morphology by SEM analysis. Bangash and Alam (2009) activated *Ailanthus altissima* wood by a physical method at a temperature of 400-800°C.

The aim of this work is to characterize the activated carbons prepared from *Acacia mangium* wood in the presence of CaO and KOH activating agents. The chemical activation effects on pore size and surface area formation (analysed with BET and DR isotherms), surface morphology (by SEM imaging technique), elemental constituents and surface functional groups (analysed by EDX and FT-IR), iodine number (analysed by iodine adsorption method), and thermal stability (analysed by TGA) have been minutely observed. The burn-off percentage and cation exchange capacity were also calculated for COAC and PHAC.

EXPERIMENTAL

Reagents and Chemical Activating Agents

Chemical activating agents as well all the reagents used in this study were of analytical grade, purchased from Sigma-Aldrich, HmbG, and Fluka Chemicals.

Preparation of *Acacia mangium* Wood Activated Carbon

Samples of *Acacia mangium* woods were collected from the campus of Universiti Sains Malaysia, cut into small pieces, and dried at 378 K for 12 hours. The samples were ground into powdered form and sieved (particle size was selected as smaller than 50 mesh and bigger than 100 mesh size) to get the proper size for uniform activation. A single-stage activation process was adopted for the production of activated carbon. Mechanically ground coarse wood-dust of *Acacia mangium* was soaked in a dilute solution of KOH and CaO in the ratio of 2:1 (weight ratio of *Acacia mangium* wood sample to activating agent; in this experiment 30 g of wood powder is mixed with 15 g of activating agents) separately for 24 hours at 348 K. This was followed by pyrolysis of the dried mixtures inside a steel-capped graphite reactor kept in the muffle furnace (Model: GT-MF; Gotech Testing Machines Inc. Taiwan) at 773 K for 2 hours.

The reactor was then cooled to room temperature, and the agglomerated (obtained in case of KOH activation; in case of CaO activation the particle size remain same as the precursors were taken) carbon materials were ground into a uniform particle size. Uniform particles of carbon materials were washed with excess demineralised water to remove the adherent activating agents and water soluble by-products that may form on the surface of activated carbon during activation. But in case of COAC it was observed that washing of post pyrolysis product with water is not enough to remove all the by-products such as calcium carbonate, calcium bicarbonate, and adherent calcium oxides, hence 5% HCl solution was used to wash the samples several times until the effervescence after adding HCl solution had ceased. The samples were then dried in an oven at 378 K for 12 hours for complete removal of the absorbed water. Dried activated carbon was kept inside a sealed glass bottles with proper label as COAC and PHAC for further analysis.

Characterization of *Acacia mangium* Wood Activated Carbon

The characterizations of the samples were carried out at their optimal working condition. The activated carbon obtained after activation can be evaluated for burn-off percentage. Burn-off is defined as the weight difference between the precursor biomass and the activated carbon, divided by the weight of the precursor biomass, with both weights on a dry basis (Reed and Williams 2004). The following relationship was used for calculating the activation burn-off of biomass derived activated carbons:

$$\% \text{ Activation burn-off} = 100 - \left[\left\{ \frac{\text{mass after activation (g)}}{\text{precursor mass (g)}} \right\} \times 100 \right] \quad (1)$$

SEM and EDX study

Morphological and elemental composition studies of the activated carbons were done with a Leo Supra 50 VP Field Emission Scanning Electron Microscope (Carl-Zeiss SMT, Oberkochen, Germany) equipped with an Oxford INCA 400 energy dispersive X-ray microanalysis system (Oxford Instruments Analytical, Bucks, U.K.) that can give SEM and EDX with the same sample. The scanning electron micrograph (SEM) of the activated carbons at bar length equivalent to 2 μm , working voltage 15 kV with 3000x magnification are shown in Fig. 1.

FTIR spectral study

The FTIR spectra of samples were recorded with an FTIR spectrophotometer Nicolet AVATAR 380 FT-IR Model, using the potassium bromide (KBr) pellet method. Oven-dried solid samples of activated carbons were thoroughly mixed with KBr in the ratio of 1:100 (weight ratio of sample to KBr). The solid mixture of activated carbon and KBr were ground to a very fine powder and then compressed at 15,000 psi (pound force per square inch) pressure to make a thin film disk for the spectra analysis. The spectra were recorded by 64 scan with 4 cm⁻¹ resolution in the fingerprint spectral region of 4000 to 400 cm⁻¹.

TGA Study

Thermogravimetric analysis of prepared activated carbons was carried out using a Perkin Elmer Pyris1 TGA thermal analyser. The heating rate was fixed at 10 K/min in the presence of nitrogen gas with flow rate of 20 ml/min. The temperature range was selected from 293.15 K to 1073.15 K to investigate the decomposition of *Acacia mangium* activated carbons.

Porosimeter study

Nitrogen adsorption isotherms were obtained at 77 K using a NOVA 2200e surface area and pore size analyzer. The specific surface area was determined by the BET and D-R isotherm equations, and the pore size distribution was calculated with the adsorption data based on original density functional theory.

Iodine number determination

The iodine number is the most fundamental parameter used to measure the activated carbon performance in terms of activity. The higher the value of iodine number, the higher will be the degree of activity of the activated carbon. Thus the iodine number was measured to evaluate the adsorptive capacity of the carbon samples produced after activation. The known amount of activated carbon was placed in a flask containing a 0.1N iodine solution, and then shaken to maintain equilibrium for 24 hours. After adsorption, the activated carbon was removed from the solution by filtration. The iodine adsorption capacity was determined from the titration of the filtrate with standard solution of sodium thiosulfate (ASTM Designation: D4607-94). The following formula is generally applied to calculate the iodine value,

$$\text{Iodine Number} = \frac{X}{m} * A \quad (2)$$

where A is the correction factor obtained after the calculation of the residual filtrate normality, m the weight of the activated carbons in gm, and X the of adsorbed iodine in milligrams,

$$X = (N_1 * 100 - N_2 * V * \frac{110}{50}) * 126.93 \quad (3)$$

where N_1 is the normality of the iodine solution, N_2 the normality of the thiosulfate solution, and V is the volume of thiosulfate solution used for titration.

Cation exchange capacity (CEC)

A modified method based on Boehm's technique was used to measure the cation-exchange capacity (CEC) of the activated carbons (Puziy et al. 2002). A weighed amount of activated carbon (0.1 ± 0.0001 g) was placed into an Erlenmeyer flask. A volume of 20 mL of 0.1 M NaOH solution was added. To attain equilibrium the flasks were shaken for 24 hours. After equilibration the NaOH concentration was measured by titration with HCl. The quantity of NaOH consumed was converted to CEC and expressed in mmol/g using the following equation,

$$CEC = \frac{(N_1 - N_2) * V}{m} \quad (4)$$

where N_1 and N_2 are the normality of the NaOH solution before and after equilibrium, respectively, V is the volume of NaOH taken in Erlenmeyer flask, and ' m ' is the mass of activated carbon used.

pH_{zpc} determination by immersion technique (IT) methods

Suspensions of 25 g/L of activated carbon mass were put into contact with 0.03 M KNO₃ solutions adjusted at pH values of 1.50, 2.01, 3.10, 4.06, 5.08, 6.33, 8.01, 10.03, and 11.50. The suspensions were agitated for 24 hours in an orbital thermostat shaker (Protech, Model:903) at 100 rpm. The change of pH (Δ pH) during equilibration was calculated, and the pH_{zpc} was identified as the initial pH with minimum Δ pH from the pH initial versus $|\Delta$ pH| plot.

RESULTS AND DISCUSSION

Carbonization Behaviour

Previous studies on the activation of wood-based activated carbons have reported separately the effect of activating agents with different activation conditions such as temperature, duration, and impregnation ratios, etc. (Patnukao and Pavasant 2008; Solum et al. 1995; Jagtoyen and Derbyshire 1998). In this study we have tried to compare the effect of activating agents under identical conditions of other variables such as temperature of activation, impregnation ratio, and particle size of precursor. The results obtained for the carbonised samples (see Table 1) indicate that at a temperature of 773 K led to the formation of activated carbon with different burn-off percentage for the COAC and PHAC. PHAC had $73.30 \pm 0.20\%$ burn-off percentage, which indicates that more volatile compounds formed with activating agents, whereas calcium oxide formed stable complexes with wood precursors; hence after pyrolysis only 33.34% volatile matter burn-off, the rest undesired matrix was strongly attached with COAC surfaces. After washing with 5% HCl solution the matrix removed and we obtained $28.73 \pm 0.93\%$ activated

carbons. In totality we lost $70.72 \pm 0.93\%$ as burn-off percentage of the biomass in the form of volatile as well as acid soluble matrix.

SEM and EDX Interpretation of COAC and PHAC

Surface morphology of the obtained activated carbon from *Acacia mangium* wood can be seen from the representative SEM images in Fig. 1.

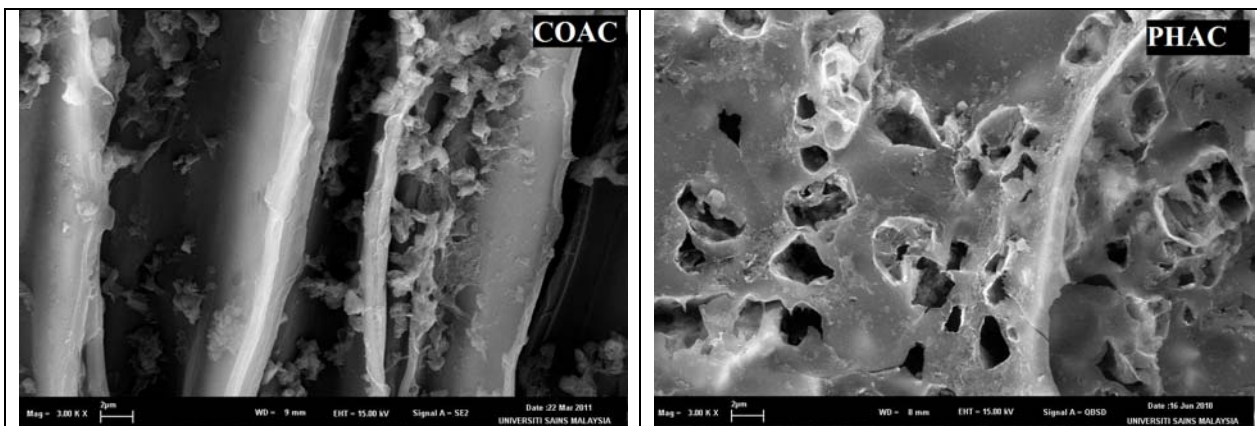


Fig. 1. SEM image of CaO activated carbon (COAC) and KOH activated carbon (PHAC) obtained from *Acacia mangium* wood powder

The SEM images exhibited irregular structure with cracks and crevices on the surface, which confirmed amorphous and heterogeneous structures. The COAC image shows no pores on the surface and reveals a sheet-like structure with troughs and crests in a synchronised manner. The interlayer gap appears to be of a few microns. The PHAC image shows partially developed honeycomb-like morphology, and some micro-holes were found on the surface. This can be explained based on an assumption that CaO may have limited accessibility to the surface of wood because of its partial soluble nature in water. Moreover, it forms large amount of matrix (undesirable compounds) with water soluble as well as surface constituents of wood that are adherent to the carbon surface. These formed stable calcium compounds on the carbon surface tend to fill interstice gaps between the layers. After activation a considerable amount of these compounds remain with the activated carbon. Washing with 5% HCl solution was effective; it had removed these matrixes and a clear inter-layered surface was seen in the corresponding SEM image. This observation is further strengthened by the EDX results in which it was found that the presence of Ca on the surface was reduced remarkably. In case of KOH activation there is no opportunity for such stable compounds to form. This hypothesis was backed up by an EDX study of the samples.

Figure 2 shows the EDX analysis of selected areas of the samples for elemental composition of the activated carbons COAC and PHAC. Figure 2[a] shows the area EDX analysis of CaO activated carbon samples. The elemental contents were 74.72% carbon, 18.89% oxygen, 2.15% chlorine and 4.24% calcium.

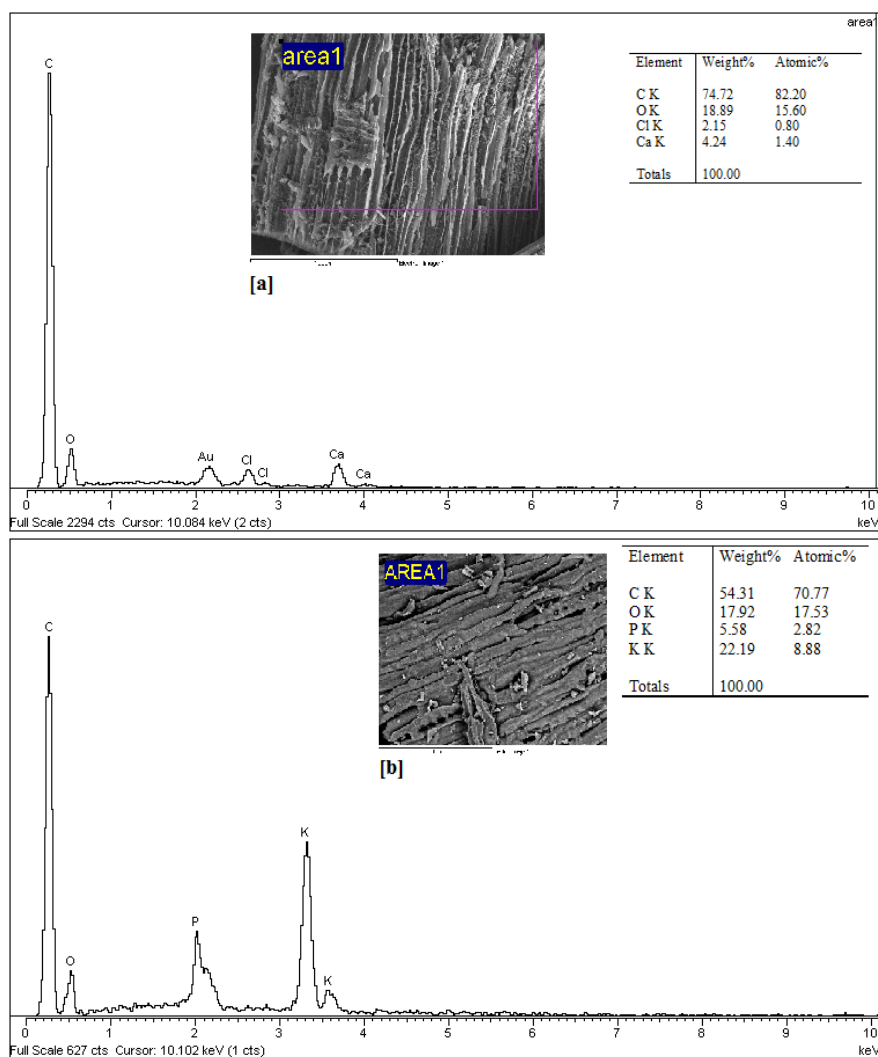


Fig. 2. EDX plot for [a] CaO activated [b] KOH activated carbons of *Acacia mangium* wood powder

Calcium oxide reacts with wood compounds to form mostly oxidative products such as calcium carbonate and calcium hydroxide; hence, the oxygen content of the formed activated carbon is less than the wood precursor (acacia mangium wood contains 48.25% oxygen by weight). Repeated washing with HCl causes some chlorine molecule to get attached with the surface of COAC, and in EDX studies their presence was also observed, even though very small percentage. On the other hand, potassium hydroxide forms a condensation product in which the potassium ion gets attached with the acidic functional group site, and water is removed from there during the formation of potassium salt of carboxylic acid as a condensation product. The KOH activated carbon contained 54.31 % carbon, 17.92% oxygen, and 22% potassium by weight, as depicted in Fig. 2[c]. This revealed that KOH activation strongly interacted with the precursor material constituent compounds. The increase of weight of potassium in the PHAC could be due to the acidic functional groups reacted with base KOH and the formation some potassium salt in the newly formed activated carbon material.

FTIR Analysis of Functional Groups in COAC and PHAC

Figure 3 represents the FTIR spectra in transmittance mode for the two activated carbons produced from *Acacia mangium* wood precursor. In the spectra of COAC before 5% HCl, the only major broad peak can be seen at 1700 to 1200 cm^{-1} with a maximum at about 1420 cm^{-1} that is characteristic of C-O stretching of perhaps carbonate, carboxylic acid, and/or ketonic groups (Coates 2000). A minor but sharp peak at 874.77 cm^{-1} supports the presence of carbonates. The next broad peak, but having low intensity, is observed at 3650-3200 cm^{-1} with a maximum at about 3407.97 cm^{-1} . This peak is due to the presence of -OH stretching in bonded and non-bonded hydroxyl groups and water molecules, for which the small intensity of the peak indicates the low content of these groups in the activated carbon(COAC). The backbone of the structure mainly containing ali-phatic carbon chains helps to explain the presence of a narrow band at 2980.01 cm^{-1} , and -CH- stretching is also present in the chain, giving an absorption band at 2873.42 cm^{-1} . Some sulphur-containing groups were also there, and its narrow and small peak can be seen at 2511.86 cm^{-1} . Another peak in the spectra at 1820-1775 cm^{-1} with a maximum of about 1796.37 cm^{-1} is due to the presence of aryl carbonate. A sharp peak at 712.16 cm^{-1} is probably due to -OH out-of-plane vibration. Overall, the calcium oxide spectrum points to the presence of mostly oxygen-based functional groups. After washing of COAC with 5% HCl solution most of the oxygen-containing peaks had disappeared from the surface, and only small peaks in the carbonyl group region remained. And few weak peaks in -CH- stretching group region remained. The carbonate peak at 874.17 had completely disappeared, which indicates that complete washing of the COAC has been achieved. Moreover, EDX analysis results also support the presence of functional atoms. For example COAC before 5% HCl washing contained 38.25% oxygen, whereas after washing it was reduced to 18.89%.

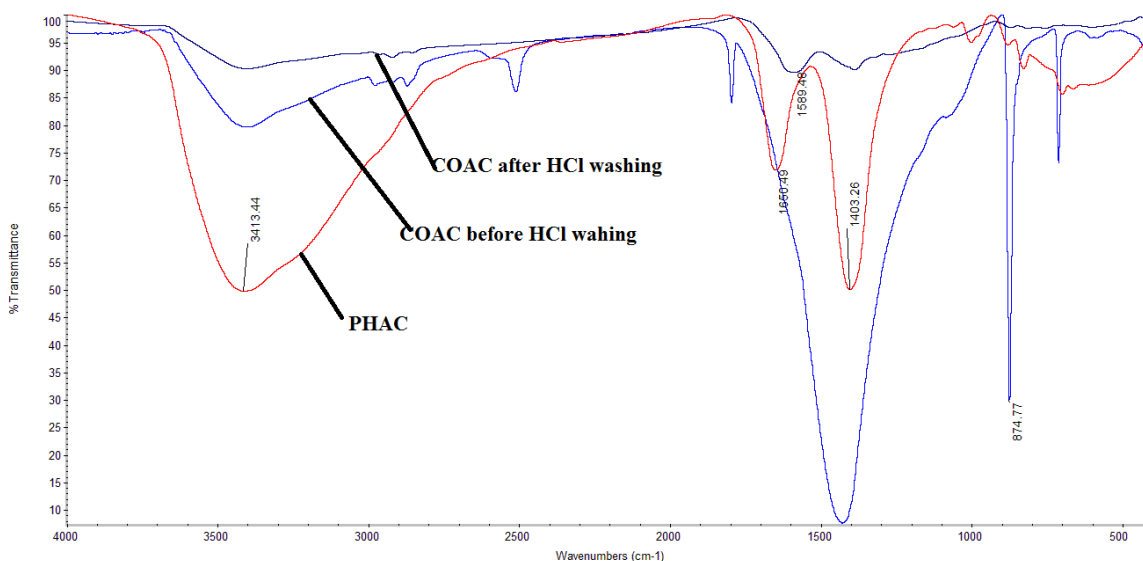


Fig. 3. Fourier transform infrared spectra of KOH & CaO activated carbons

In the spectrum of PHAC, three major broad peaks can be seen, as shown in Fig. 3. The first broad peak at 3700-2700 cm^{-1} with a maximum at 3405.62 cm^{-1} is characteristic of $-\text{OH}$ stretching vibration of the hydrogen bonded hydroxyl groups from carboxyl, phenol, and alcohols. The second major peak is at 1480-1300 cm^{-1} with a maximum at 1401.97 cm^{-1} . This peak implies the presence of salt of carboxylate, probably the potassium salt of carboxylate. A third broad peak is at 1700-1530 cm^{-1} with a maximum at 1650.40 cm^{-1} , indicating the presence of $-\text{NH}$ stretching of a secondary amine group. These spectra also show small intensity peaks in the main fingerprint spectral region between 1200 and 600 cm^{-1} with maxima at 1061.72, 1002.28, 879.62, 826.56, 699.51, and 664.86 cm^{-1} , indicating the presence of $-\text{CO}$ stretching of secondary alcohol, $-\text{CH}_2-$ stretching of cyclohexane ring, aromatic C-H out of plane bend, and C-Br stretching, respectively.

TGA Analysis of COAC and PHAC

Thermogravimetric analysis (TGA) was used to characterize the thermal stability of the prepared activated carbons. The mass loss of the material was calculated against the temperature rise. Figure 4 shows TGA curves of the two activated carbons.

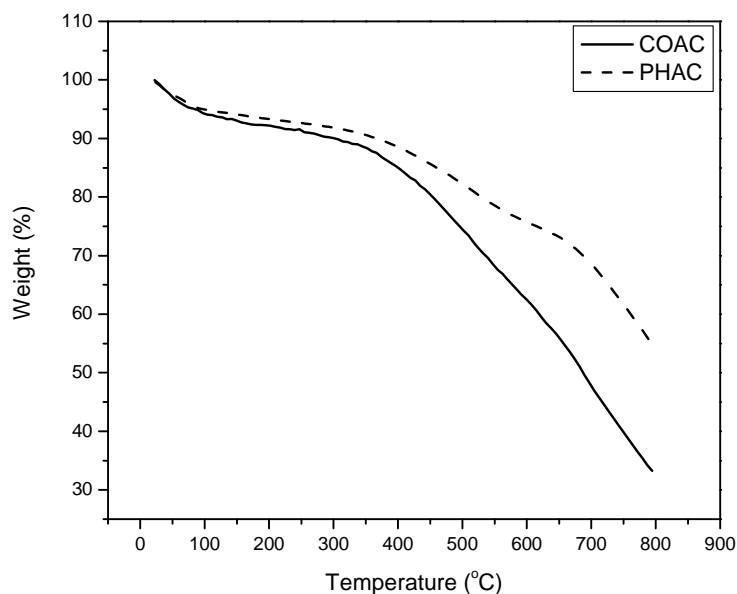


Fig. 4. [a] TGA plot of KOH- (dotted lines) and CaO- (solid lines) activated carbons

It can be seen that the calcium oxide-activated carbon (COAC) exhibited two onset temperatures, first at a temperature of about 632.26 K with a percent mass loss 7.35%, and second onset at a temperature of 926.32K with a percent mass loss 43.11%. This implies that COAC initially loss around 7.35 wt.% at lower temperature is due to the presence of some hygroscopic molecules like water. Losses around 43.11 wt.% at 926.32 K are probably due to loss of carbon dioxide and carbon monoxide from the COAC, which may remain unburned or partially burned during pyrolysis activation. In the TGA plot (Fig. 4) the dotted line curve represents the PHAC degradation trend; note that this

curve also exhibited two onset points. First onset was observed at a temperature of 662.12 K with a mass loss around 8.17%, and the second onset was at a temperature of 940.47 K with a mass loss 26.867%. This implies that the initial loss of weight is very close to COAC, and it also seems to be due to loss of moisture. The second onset loss of 26.867% by weight implies that PHAC becomes stabilized during pyrolysis, with only 26.867% remaining as unburned or partially burned matter that may escape from the PHAC in the form of carbon dioxide and carbon monoxides at 940.47 K. Hence, it can be deduced from this study that *Acacia mangium* KOH activated carbon has better stability at temperatures up to 1073.15 K.

Pore Size Distribution Study

Activated carbon is known to possess a complex porous structure. Further information on pore structure could be obtained from a nitrogen adsorption-desorption isotherm, as shown in Fig. 5. The graph shows selected adsorption-desorption isotherms of N_2 at 77 K. Prior to the N_2 adsorption isotherm experiment the samples were degassed at a temperature of 393.15 K. The physi-sorption isotherms can be classified based on the schemes for type-I to type-VI curves, according to the International Union of Pure and Applied Chemistry (IUPAC) system of nomenclature. In most of the cases at sufficiently low surface coverage the isotherm reduces to a linear form, which is often referred to as the Henry's law region. The isotherms obtained for both the activated carbons belonged to the reversible type-II, which is the normal form of isotherm obtained with a non-porous or macroporous material. The obtained isotherms hysteresis plots for COAC and PHAC were almost similar to the H3 hysteresis plot of IUPAC nomenclature. The characteristics features of H3 loop materials are that they do not exhibit any limiting adsorption at high P/P_0 . Such behaviour is characteristic of aggregates of plate-like particles giving rise to slit-shaped pores (Sing et al. 1985).

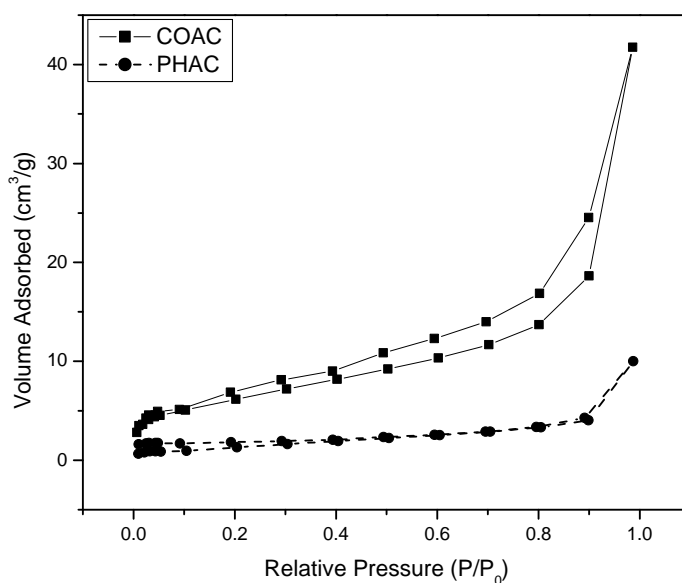


Fig. 5. Nitrogen adsorption-desorption isotherm at 77K for COAC and PHAC

Figure 6 shows the pore size distribution calculated by the BET isotherm for both the activated carbons. Pore characteristics as well as surface area of both COAC and PHAC are reported in Table 1. The higher BET specific surface area obtained for calcium oxide-activated carbon may be explained on the basis of carbon content of the activated carbons (74.72% by weight carbon present in CaO-activated, 54.31% by weight carbon present in KOH-activated carbons); a higher carbon content of COAC can lead to the formation of a good grapheme-like layered structure (as seen in SEM image) that can generate higher surface area than the non-layered structure (in case of PHAC). In chemical activation by KOH and CaO, the chemical activating agent is introduced into the wood precursor, resulting in physical and chemical changes and modifying the thermal degradation process. During the soaking period at mild heat the activating agents function in two ways; first they act as a basic catalyst for wood precursor to promote the bond polarization; second they act by combining with the acidic sites, promoting condensation reactions and removing small molecules such as water and carbon dioxide in the case of KOH. But CaO mainly oxidises the surface of the precursor and may form the metal organic dative bonds, which can connect and crosslink biopolymer fragments. During pyrolysis activation lot of CO₂ is formed inside the closed graphite reactor, and the diffusion of the oxidating agent through the carbonaceous matrix involves the removal of impurities and the consumption of carbon to create porosity according to the following reaction (Phan et al. 2006):

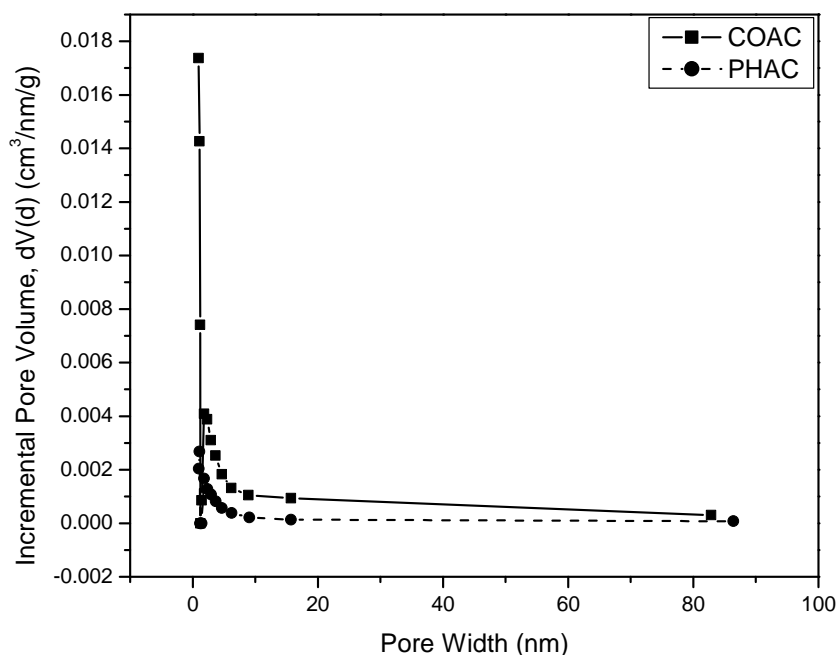


Fig. 6. Pore width versus Incremental pore volume plot for COAC and PHAC

The microporosity is opened and widened into mesoporosity as the removal of the exterior of the particle is significant at high burn-offs (Rodriguez-Reinoso et al. 1992). The different mechanisms mean that chemical activation produces, in one step, a large yield of activated carbon having a micropore structure as well developed as in the CO₂ gasification, with the advantage of a larger mesopore volume and a lower micropore volume. The microporous volume of COAC and PHAC calculated by DR isotherm was 0.0511 and 0.004 cm³/g, respectively. It may be noted that activated carbon of *Acacia mangium* prepared from CaO activation had a higher specific surface area and microporosity percentage than KOH activated carbon. This may be due to the higher oxidation of precursor wood by CaO, which influences the generation of microporosity on the surface of activated carbon generated.

Effect of Activating Agents On Iodine Number, CEC and pH_{zpc}

Iodine number is an indication of the adsorption capacity in micropores; therefore, it is often employed to examine the adsorption capacity of the activated carbons by contemporary researchers. Table 1 summarises the iodine values for COAC and PHAC. A higher value of iodine number for COAC is due to greater surface area and available micropores for adsorption of iodine molecule at the surface. On the other hand, a low iodine value of PHAC can be due to lack of appropriate surface area and micropores at the surface; rather, it forms a macro porous structure. A sheet type layer structure of COAC with high micropores volume was also supported by the shape of the N₂ adsorption isotherm plot.

Table 1. Textural Parameter Deduced from N₂ Adsorption at 77 K on Activated Carbons COAC and PHAC

Parameters		Activated carbon	
		COAC	PHAC
S _{BET} (m ² /g)		65.53	5.253
Total pore Vol.(cm ³ /g)		0.090	0.015
Av. Pore Dia.(nm)		5.509	11.79
t-method	S _{ext.} (m ² /g)	65.53	5.253
	V _{micropor.} (cm ³ /g)	0.0002	0.0168
DR method	S _{microp.} (m ² /g)	144.00	11.47
	V _{microp.} (cm ³ /g)	0.0511	0.004
Iodine number		319.67±6.23	286.26±8.75
pH _{zpc}		6.08	7.20
Cation exchange capacity (mmol/g)		4.97±0.23	2.79±0.16
Burn-off (%)		70.27±0.93	73.30±0.20

Any positively charged ions on the surface of activated carbons are called cations, in the present case, and these may be basic cations like calcium (Ca^{2+}) and/or potassium (K^+), or they can be the acidic cation hydrogen (H^+). The amount of these positively charged cations hold on the surface of activated carbons is described as the CEC and is expressed in terms of mmol/g. The larger is the cation exchange capacity, the more cations can be held at the surface of activated carbon. In the present study COAC exhibited a CEC of 4.97 ± 0.23 mmol/g, whereas PHAC had a CEC of only 2.79 ± 0.16 mmol/g. It can be inferred from this study that COAC had a better cation holding capacity, which could be due to the presence of initial divalent calcium ions replaced by the protons during HCl washing. Each of these divalent ions of calcium can be replaced by two units of univalent ions, and these cations may be the hydrogen ions.

The significance of pH_{Zpc} of a given activated carbon surface is that it will have a positive charge at solution pH less than their pH_{Zpc} and thus be a surface on which anion may adsorb. On the other hand, if the solution pH has greater than that of pH_{Zpc} of activated carbon, the carbon surface will bear negatively charged, and cations may adsorb on the surface. The pH_{Zpc} of COAC and PHAC were found to be 6.08 and 7.20 respectively, which can be interpreted in terms of a negatively charged surface for activated carbons in the basic range (pH > 7.2) of solution. It follows that COAC and PHAC are suitable of cationic pollutants removal in basic solution ((pH > 7.2)).

CONCLUSIONS

1. Investigation of CaO and KOH activated carbons helped to elucidate the production of two different kinds of activated carbons, where COAC has a sheet-like morphology, whereas PHAC is comprised of underdeveloped micro-porous carbon. Both activating agents have almost equal percentage of oxygen by weight, but form major difference in surface functional groups as evident by FTIR spectra. The COAC showed no major peak in the bonded and non bonded —OH group region, whereas PHAC exhibited a strong peak in this region.
2. It was observed that COAC had a more acid-soluble matrix within the carbon framework. By contrast, in PHAC mostly volatile matrixes are formed during activation, and these volatile components are mostly lost from the carbon network during pyrolysis. PHAC forms thermally stable activated carbon compared to COAC.
3. It can be concluded from this study that chemical activation is a suitable method for getting new activated carbon materials. It was also observed that material produced with the same precursor, under identical activation condition, has a big impact of chemical activating agents on the surface functional groups, pore formation, and thermal stability of the new material.

ACKNOWLEDGMENTS

The authors acknowledge the Research University Postgraduate Research Grant Scheme (1001/PTEKIND/844042) for funding the research and Universiti Sains Malaysia for the Fellowship provided to Mohammed Danish.

REFERENCES CITED

- Bangash, F. K., and Alam, S. (2009). "Adsorption of Acid blue 1 on activated carbon produced from the wood of *Ailanthus altissima*," *Braz. J. Chem. Eng.* 26(2), 45-53.
- Bansal, R. C., Donnet, J. B., and Stoeckli, H. F. (1988). *Active Carbon*. Marcel Dekker Inc., New York.
- Benaddi, H., Bandosz, T. J., Jagiello, J., Schwarz, J. A., Rouzaud, J. N., Legras, D., and Béguin, F. (2000). "Surface functionality and porosity of activated carbons obtained from chemical activation of wood," *Carbon* 38(5), 669-674.
- Bota, A., Laszlo, K., Nagy, L.G., and Schlimper, H. (1997). "Active carbon from apricot pits," *Magyar Kemiai Folyoirat* 103(9), 470-479.
- Coates, J. (2000) *Encyclopedia of Analytical chemistry*, Meyers, R. A. (ed.), John Wiley and Sons Ltd., Chichester.
- Danish, M., Sulaiman, O., Rafatullah, M., Hashim, R., and Ahmad, A. (2010). "Kinetics for the removal of paraquat dichloride from aqueous solution by activated date (*Phoenix dactylifera*) stone carbon," *Journal of Dispersion Science* 31(2), 248-259.
- Hameed, B. H., Ahmad, A. A., and Aziz, N. (2007). "Isotherm kinetics and thermodynamics of acid dye adsorption on activated palm ash," *Chemical Engineering Journal* 133(1-3), 195-203.
- Jagtøyen, M., and Derbyshire, F. (1998). "Activated carbons from yellow poplar and white oak by H₃PO₄ activation," *Carbon* 36(7-8), 1085-1097.
- Kumar, S., Rajmohan, B., Mohanty, K., and Meikap, B.C. (2010) "Characterisation of activated carbon prepared from tamarind wood for wastewater treatment," *International Journal of Environmental Engineering* 2(1-3), 290-302.
- Lee, W. H., and Reucroft, P. J. (1999) "Vapor adsorption on coal-and wood-based chemically activated carbons(II) adsorption of organic vapors," *Carbon* 37, 15-20.
- Moreno-Pirajan, J. C., and Giraldo, L. (2010). "Study of activated carbons by pyrolysis of cassava peel in the presence of chloride zinc," *J. Anal. Appl. Pyrolysis* 87(2), 288-290.
- Patnukao, P., and Pavasant, P. (2008). "Activated carbon from *Eucalyptus camaldulensis* Dehn bark using phosphoric acid activation," *Bioresource Technology* 99, 8540-8543.
- Phan, N. H., Rio, S., Faur, C., Coq, L. L., Cloirec, P. L., and Nguyen, T. H. (2006). "Production of fibrous activated carbons from natural cellulose (jute, coconut) fibers for water treatment applications," *Carbon* 44(12), 2569-2577.
- Puziy, A. M., Poddubnaya, O. I., Martínez-Alonso, A., Suárez-García, F., and Tascón, J. M. D. (2002). "Synthetic carbons activated with phosphoric acid. I. Surface chemistry and ion binding properties," *Carbon* 40, 1493-1505.

- Reed, A. R., and Williams, P. T. (2004). "Thermal processing of biomass natural fiber wastes by pyrolysis," *Int. J. Energy Res.* 28, 131-145.
- Sing, K. S. W., Everett, D. H., Haul, R. A. W., Moscou, L., Pierotti, R. A., Rouquerol, J., and Siemieniewska, T. (1985). "Reporting physisorption data for gas/solid systems with special reference to the determination of surface area and porosity," *Pure & Appl. Chem.* 57(4), 603-619.
- Solum, M. S., Pugmire, R. J., Jagtoyen, M., and Derbyshire, F. (1995). "Evolution of carbon structure in chemically activated wood," *Carbon* 33(9), 1247-1254.

Article submitted: February 19, 2011; Peer review completed: March 21, 2011; Revised version received: April 23, 2011; Accepted: June 21, 2011; Published: June 23, 2011.